3 EXPERIMENTAL

3.1 Catalyst preparation

Supported cobalt catalysts (9 wt% Co) were prepared by incipient wetness impregnation /31/ of γ-Al_2O_3 with an aqueous solution of $Co(NO_3)_2$. 0.9 - 1.1 ml of the aqueous solution was used per gram of alumina support under impregnation. Bimetallic catalysts were prepared by addition of 0.1 - 1 wt % of Pt, Re, Ru, Ir or Pd. Table 3-2 shows the different catalysts, their metal precursors, composition after calcination and calcination temperature.

Two different commercial γ-aluminas, but with similar specifications, were used as supports. The first was "Alumina 000 - 1½ E" from Akzo and is recognized by an "A" in the end of the catalyst name. This support was received as pellets which were crushed and sieved to particle size 52 to 200 mesh (75 -300 µm). The other support was Vista Boehmite Alumina from Vista Chemical Company, received as a powder. The same fraction of particles as mentioned above was used from this support. The Vista support is recognized by a "B" in the end of the catalyst name.

The bimetallic catalysts with the Akzo support were all made by sequential impregnation, and the catalysts were calcined between each impregnation step. Cobalt was always added first. The bimetallic catalysts with the VistaB support were made by coimpregnation.

After impregnation the catalysts were dried overnight in air at about 400 K. The catalysts were calcined in flowing air (5 Nml/min·g catalyst) at temperatures between 573 K and 698 K for two hours. The unpromoted cobalt catalyst on support A was calcined a second time in order to have the same treatment as the bimetallic, sequentially impregnated catalysts.

The catalysts were after calcination again sieved to particle size 52 to 200 mesh.

A Co_3O_4 bulk catalyst was prepared by precipitation by adding NH_3 to an aqueous solution of $Co(NO_3)_2{*}6H_2O$ with continuous stirring until there were an excess of NH_3. The

precipitate was washed several times in distilled water and dried overnight at 370 K. Calcination was done in flowing air at 643 K or at 698 K for three hours.

BET-surface and pore size measurements were performed at SINTEF Applied Chemistry, and data for the calcined cobalt catalysts on the two supports are shown in Table 3-1 and Appendix 5. XRD measurements were performed at Department of Physical Chemistry, NTH.

Table 3-1. BET surface and pore size data[a].

	Co/Al_2O_3A	Co/Al_2O_3B
Specific surface area (m^2/g)	176	179
Pore radius (Å)	30 - 60	30 - 60
Pore volume (Nml/g)	0.4	0.4

[a] Measured at SINTEF Applied Chemistry.

More detailed information about all chemicals, supports, gases and catalysts mentioned in this chapter are given in Appendix 1 and 2.

Table 3-2. Catalysts used in the investigations.

Catalyst[a]	2nd metal precursor[b]	Co loading (wt %)	2nd metal loading (wt %)	Calcination temperature (K)
Co/Al_2O_3A		8.7		673
Co/Al_2O_3B		8.5 8.7 8.7		573 648 698
$Co0.1Pt^*/Al_2O_3A$	$H_2PtCl_6{}^*6H_2O$	8.7	0.1	673
$Co1.0Pt^*/Al_2O_3A$	$H_2PtCl_6{}^*6H_2O$	8.7	1	673
$Co0.5Pt/Al_2O_3A$	$Pt(NH_3)_4(NO_3)_2$	8.7	0.5	673
$Co1.0Pt/Al_2O_3A$	$Pt(NH_3)_4(NO_3)_2$	8.7 8.7	1 1	643 673
$Co1.0Pt/Al_2O_3B$	$Pt(NH_3)_4(NO_3)_2$	8.5 8.7	1 1	573 648
$Co0.1Re/Al_2O_3A$	Re_2O_7	8.7	0.1	673
$Co1.0Re/Al_2O_3A$	Re_2O_7	8.7	1	673
$Co1.0Re/Al_2O_3B$	Re_2O_7	8.5	1	573
$Co0.1Ir/Al_2O_3A$	$H_2IrCl_6{}^*6H_2O$	8.7	0.1	673
$Co0.1Pd/Al_2O_3A$	$PdCl_2$	8.7	0.1	673
$Co0.1Ru/Al_2O_3A$	$RuCl_3$	8.7	0.1	673
Co_3O_4[d]		73		648 698
$0.3Pt^*/Al_2O_3$[c]	$H_2PtCl_6{}^*6H_2O$[c]		0.3	648

[a] Designations for the catalysts used in this report.
[b] $Co(NO_3)_2{}^*6H_2O$ is used in all catalysts in addition to the precursors mentioned.
[c] This catalyst is without cobalt.
[d] Unsupported catalyst.

3.2 Temperature programmed reduction

3.2.1 Principles

When using temperature programmed analysis the catalysts can be studied under conditions close to the catalytic reaction system conditions. In temperature programmed reduction, TPR, /56/ a catalyst precursor containing oxygen undergoes a programmed temperature rise while being exposed to a reducing gas, usually hydrogen diluted by an inert gas. A general equation for the reduction can be written

$$MO\ (s) + H_2\ (g) \rightarrow M\ (s) + H_2O\ (g)$$

The reduction rate is measured continuously by monitoring the composition of the reducing gas at the outlet of the reactor. Peaks appear when the reduction rate passes through a maximum. The interpretation of the TPR spectra is usually confined to the discussion of peak maximum temperatures, the number of (more or less resolved) peaks and to the total reactant consumption from which the extent of reduction can be determined. Shifts in peak temperatures depend among other factors on metal - support interactions, metal - metal oxide interactions and on metal oxide particle size. The shape and position of the TPR profiles will also be affected by readsorption, mass transfer effects, subsurface H_2 diffusion and surface heterogeneity /69/. Determination of the hydrogen consumption in the TPR runs can be done by calibration with a completely reducible metal oxide with a well defined composition.

In addition, in temperature programmed analyses there will be experimental parameters that will influence the resulting spectra. Some of these parameters are /69,95/

- Gas flow rate.
- Reactant gas/inert gas ratio: An increase of reactant concentration in the reactor will give lower peak temperatures.
- Heating rate: Increasing rate gives a shift to higher peak temperatures, sharper peaks, but lower resolution. Low heating rate will give better resolution, but broader peaks.
- Catalyst sample mass/volume: Resolution of two separate reduction processes decreases with increasing mass and the peaks will shift to higher temperatures.
- Catalyst sample particle size and geometry
- Geometry of the reaction vessel

- Signal intensity
- System pressure

The last four points are all important, but it is difficult to predict in what way changes will influence the spectra. Experience with the specific apparatus are both useful and necessary. Some care must therefore be taken when comparing the results obtained in different laboratories.

3.2.2 Apparatus and procedure

A standard apparatus, like the Rogers-Amenomiya-Robertson arrangement /70/, built at NTH by S. Vada /88/ was used for the temperature programmed reduction (TPR) investigations. A schematic drawing of the apparatus is shown in Figure 3-1. Both temperature programmed methods and pulse adsorption can be performed with the apparatus.

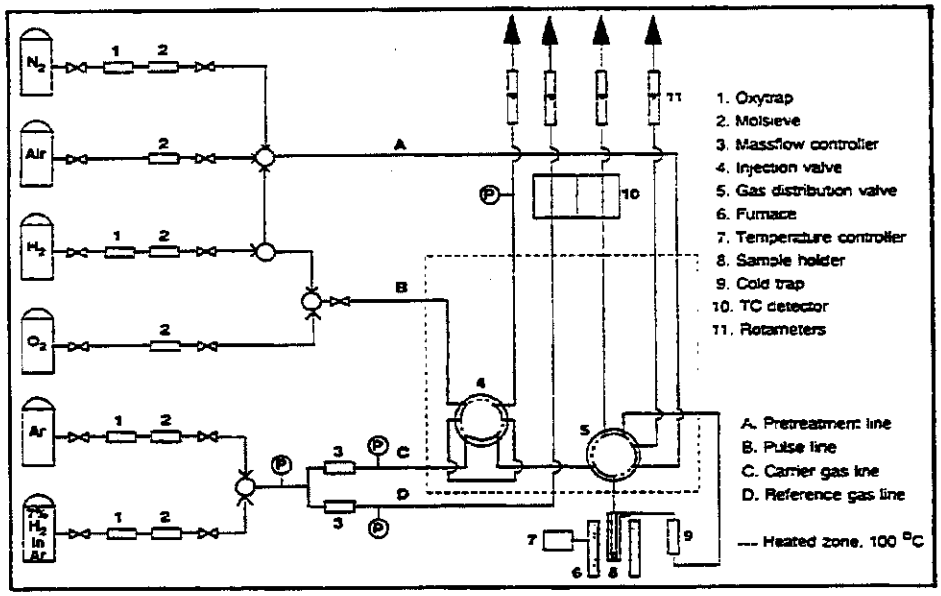

Figure 3-1. Outline of the combined temperature programmed analyses and pulse apparature.

The experimental unit consists of

- a section for feeding and dosing treatment and adsorption gases, with Alltech molsieves and oxytraps for gas purification and with Hi-tec F-100/200 massflow meters/controllers.
- a quarts glass sample holder which is shaped with an inner and an outer tube, where the sample is placed on a quarts frit in the bottom of the inner tube.
- a detection unit with a TC detector in a Shimadzu GC-8A gas chromatograph connected to a Shimadzu C-R5A Chromatopac integrator.
- a vertical electrical Kanthal furnace controlled by a Eurotherm 818P temperature controller.
- two thermocouples: one is placed in the sample holder immediately above the sample, measuring the temperature on the gas reaching the sample. The other thermocouple is used for furnace control, and is placed outside the sample holder.

The incoming gas is preheated by the gas leaving the sample holder by passing between the tubes. After the sample holder the gas passes through a cold trap (195 K) for removal of water and other condensables.

Standard conditions for the TPR experiments were:

Mass of catalyst:	0.2 g of supported catalysts
	0.02 g of unsupported catalysts
Temperature interval:	300 - 1173 K
Heating rate:	2 or 10 K/minute
Reducing gas:	7 % H_2 in Ar
Gas flow rate:	30 ml/minute
Pressure:	1 bara

Hydrogen consumption was calculated after calibration with silver oxide, Ag_2O. Ag_2O is assumed to be reduced 100 % to silver metal, showed by a single peak in TPR.

A new calibration was done for each choice of heating rate.

3.3 Pulse O_2 titration

3.3.1 Principles

Pulses of oxygen are injected into a flow of inert gas over the reduced catalyst. Knowing the pulse volume and the number of pulses consumed, the amount of gas reacted to form a metal oxide, can be calculated.

This technique is suitable for measurements of the degree of reduction by injecting oxygen on reduced samples at temperatures high enough for complete oxidation /36,73/.

3.3.2 Apparatus and procedure

The same experimental unit as used for the TPR investigations (Figure 3-1) was used for the pulse O_2-titration. A loop for pulse injections is connected to the carrier gas stream before the catalyst sample holder. The loop volume used for O_2 titration was 0.05 ml. The oxidation can with the available apparatus be done at temperatures in the range 200 to 1200 K.

The carrier gas used was argon. Standard pretreatment of the catalysts before pulse O_2-titration was reduction in hydrogen at 623 K for 16 hours. Before O_2 titration the catalysts were flushed with argon, one hour at reduction temperature (623 K), during heating to 673 K with 5 K/min heating rate and for ten minutes at 673 K. Oxygen titration was done at 673 K, and 20 to 35 pulses were injected to 0.05 g samples.

The apparatus was also used for passivation of reduced catalysts as a pretreatment for XRD investigations: The reduced catalyst was in this case cooled to room temperature in argon and flushed for 30 minutes before oxygen was pulsed on the catalysts.

3.4 Volumetric chemisorption of H_2 and CO

3.4.1 Principles

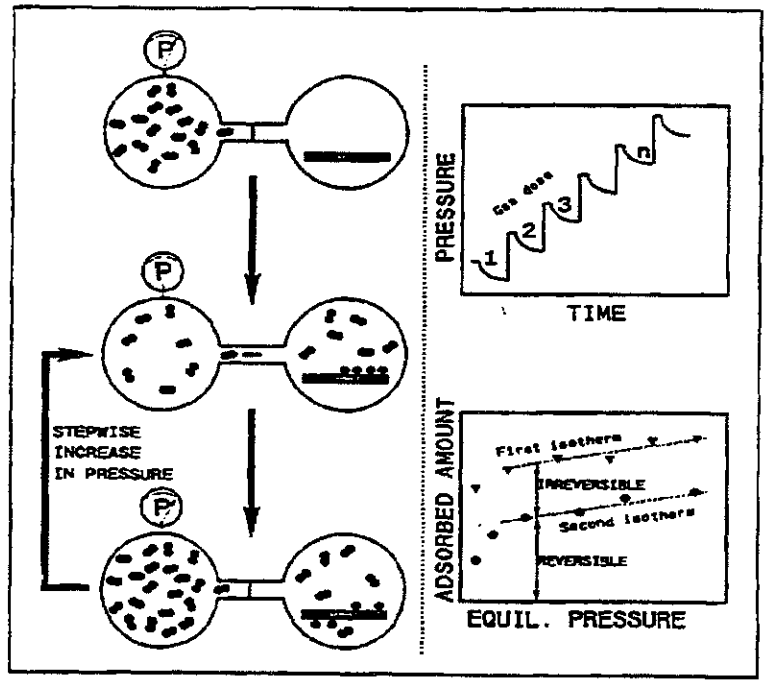

Figure 3-2. Outline of a volumetric chemisorption apparatus/measurement. From Bergene /57/.

The principle for this method is to measure the adsorbed amount of gas as a function of pressure, and thus generate an adsorption isotherm. This is done by recording the pressure decrease when a known amount of gas expands into a known volume with the sample in it, as shown in Figure 3-2 (Bergene /57/). In this work the adsorption method is used; that is measuring the isotherm in increments of increasing pressure.

The adsorbed amount corresponding to one monolayer is determined by extrapolating the linear part of the isotherm (100 to 300 torr) to zero pressure. It is customary to measure two isotherms with evacuation in-between. The second isotherm, giving the amount of weakly adsorbed gas or the "reversible" fraction, is subtracted from the first isotherm (the total adsorbed amount) to get the amount of strongly or "irreversibly" adsorbed gas /57/.

The adsorption stoichiometry for H_2:Co is assumed to be 1:2, and for CO:Co it is assumed to be 1:1 /142/. These assumptions make it possible to calculate the dispersion (the ratio between the number of the atoms exposed at the surface and the total number of metal atoms present in the catalyst) of the metal.

3.4.2 Apparatus and procedure

Figure 3-3 gives an outline of the chemisorption unit /57/. The unit is a conventional glass apparatus with greased stopcocks and a Hg diffusion vacuum pump, designed according to ASTM Standard D-3908-82 /59/. The pressure in the cell is monitored by the electronic pressure gauge, which is regularly calibrated against a Mensor quarts-spiral pressure gauge.

1 g of calcined catalysts was heated in flowing hydrogen (150 Nml/min) with a heating rate of 2 K/min. from room temperature, and reduced in situ at 623 K for 14 to 16 hours. After reduction the sample cell was cooled to 603 K and evacuated to a pressure below 10^{-5} torr before cooling to 298 K, which was the adsorption temperature. After hydrogen was admitted to the sample the equilibrium pressure for the first step was reached after 1-2 hours. For the next steps equilibrium was reached after about 15 minutes. A stepwise increase in pressure was continued until the equilibrium pressure reached approximately 350 torr. Then the sample was evacuated to 10^{-5} torr for 10 - 120 minutes before the second isotherm was recorded in a similar way. When the amount of weakly chemisorbed gas on different catalysts is compared, the same evacuation time is used for all catalysts, about 20 minutes.

After finishing the chemisorption experiment, the dead space was measured by filling the cell with a known amount of helium and measuring the pressure.

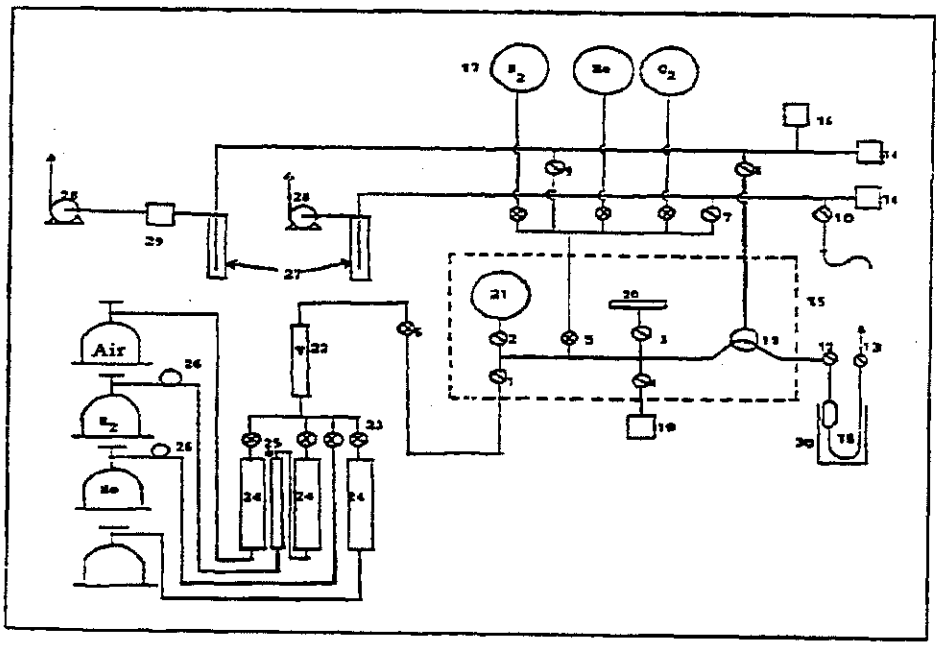

1–4: Glass stopcocks
5: Glass/PTFE stopcock
6: Needle valve
7–13: Glass stopcocks
14: Low–vacuum gauge
15: Parts kept at 298±0.1 K
16: High vacuum gauge
17: Gas reservoirs
18: Adsorption cell
19: Quarts spring pressure gauge
20: Electronic pressure gauge
21: Calibrated volume
22: Gas flow meter
23: Gas inlet valves
24: Gas purifier
25: Indicating oxytrap
26: Oxytrap
27: Liq. N_2–cooled trap
28: Rotary vacuum pump
29: Hg–diffusion pump
30: Furnace

Figure 3-3. Volumetric chemisorption apparatus. From Bergene /58/.

3.5 Kinetic investigations

3.5.1 Apparatus and analytical equipment

The kinetic experiments were done in a stainless steel fixed-bed microreactor. The complete apparatus is shown in Figure 3-5.

The total length of the reactor is 45 cm and the inner diameter is 1.12 cm. The catalyst sample is placed on a frit 11 cm from the reactor bottom. The reactor was heated by a Kanthal furnace, and the temperature was regulated by a programmed West 2050 temperature controller (TC) connected to a thermocouple placed ca. 0.5 cm below the catalyst bed. The temperature in the catalyst bed was monitored by a movable thermocouple placed into the catalyst bed. This part of the reactor is shown in Figure 3-4.

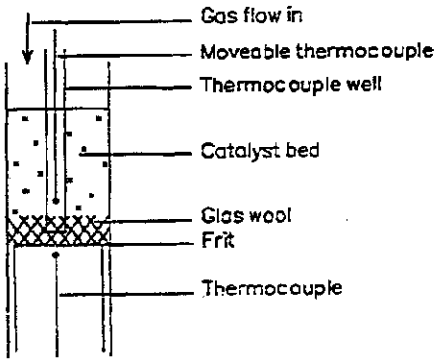

Figure 3-4. Drawing of the catalyst bed.

The apparatus is built for pressures in the range 1 to 12 bar. The reactor pressure is regulated by a Hi-Tec Pressure controller (PC).

Three parallel feed gas lines with respectively CO, He and H_2 are connected to the reactor. Each feed line is equipped with an Alltech oxytrap and molsieve, and the flows are regulated by Hi-Tec F-100/200 mass flow controllers (MFC).

The product line is split into a heated line (423 - 473 K) for analysis on the flame ionization detector (FID), and a cold line for thermal conductivity detector (TCD) analyses. The cold line passes through a condensation box for removal of the condensible gases. Product and feed gases were analyzed by a HP5890 gas chromatograph with a HP3393A integrator. The TCD was connected to a column of type Carbosieve -SII, 1/8" 110/120 (Supelco) separating

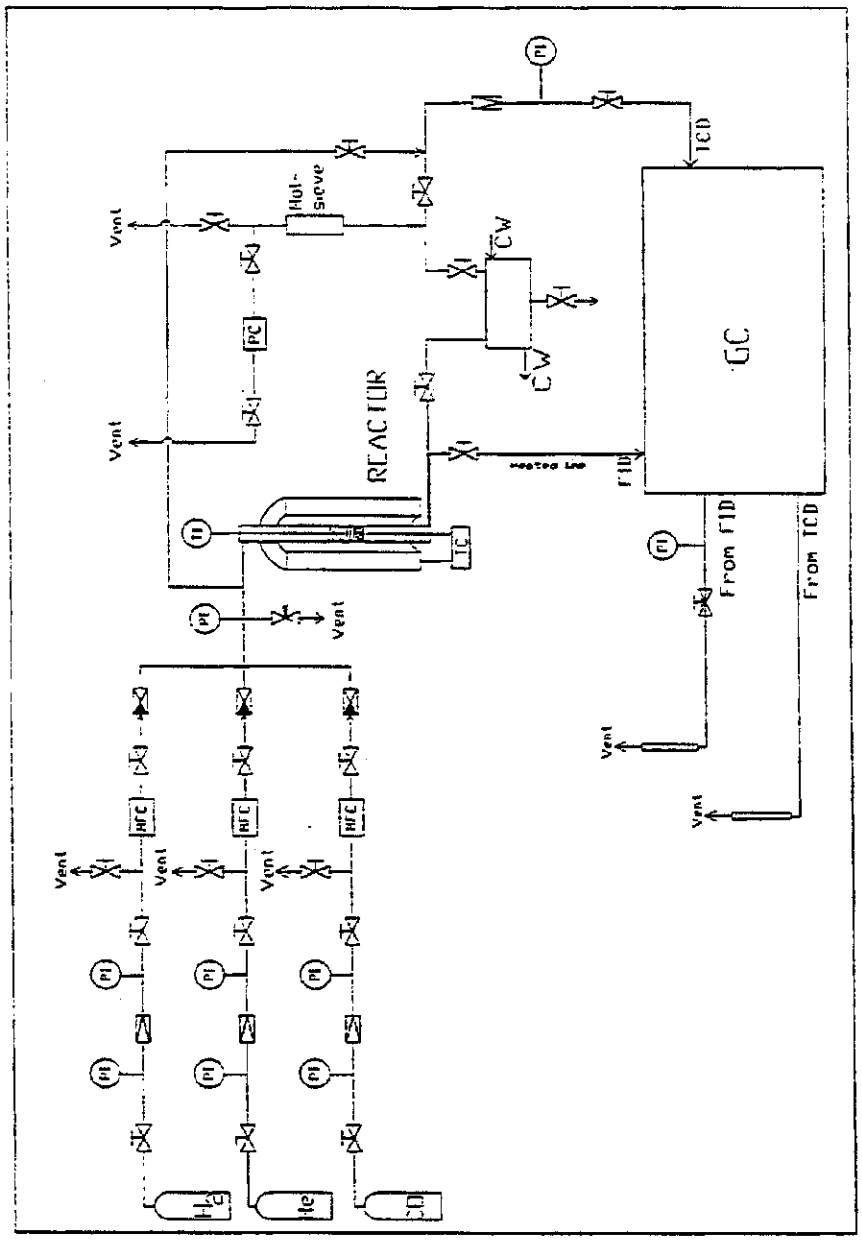

Figure 3-5. Outline of the apparatus used for kinetic investigations.

N_2, CO, CH_4 and CO_2. The FID was connected to a Megabore 30m DB1, 5 µm film, column (J&W Scientific) separating hydrocarbons (C_1 - C_{21}).

The carrier gas for both columns was helium, purified by Chrompack oxygen and moisture filters. The CO feed contained 7.5 % premixed N_2 as an internal standard for calculations of the CO conversion and the CO_2- and CH_4-selectivity.

The hydrocarbon selectivity reported for the high temperatures/high pressure experiments was found from the FID analyses directly. The areal% in the chromatograms was assumed to equal the carbon%. Due to increasing and more pronounced condensation problems, the hydrocarbon selectivity for the low temperature and pressure experiments was found by combination of the TCD and the FID analysis data: The CH_4 selectivity was found from TCD. This value was then used in correction of the C_2 - C_4 fraction in the FID chromatogram. The C_{5+} fraction was calculated by subtracting the C_1 - C_4 fraction from 100 %. The equations used in the calculation of activity and selectivity is shown in Appendix 6.

3.5.2 Procedure for kinetic experiments

0.3 - 1.0 gram of catalyst and 3 - 5 gram of inert α-Al_2O_3 were mixed and placed between two layers of glass wool on the frit in the reactor. The particle size of both the catalyst and the diluent was 52 - 200 mesh. The catalyst was flushed with helium for approximately half an hour at room temperature and atmospheric pressure before changing the pressure to the reduction pressure (7 bara). The apparatus was then leakage tested.

After leak testing the gas flow was switched to pure hydrogen, and for reduction the flow was 300 ml/min. The heating rate was 2 K/min up to 603 K and 1 K/min from 603 K to 623 K, which was the reduction temperature for all the kinetic experiments. The reduction time was 16 hours, and after reduction the reactor was cooled down to 463 K, still with flowing hydrogen.

A careful initiation of the CO hydrogenation was practiced due to problems with run-away because of the exothermity of the reaction /89/. At 463 K CO and hydrogen was diluted 1 : 1 with helium. The helium was gradually removed over a period of 20 - 30 minutes. Then the reaction mixture was heated to the chosen reaction temperature using a heating rate of 1 K/min.

The standard H_2/CO ratio used was 2/1. but in some experiments it was varied in the range 1/1 - 4/1 in order to measure the reaction order in H_2 and CO. The temperature was varied between 473 and 529 K. and the total pressure range was 1 - 9 bar. Usually only one reaction temperature and one pressure was investigated in each experiment. The gas hourly space velocity was varied in the range 4500 - 140 000 h^{-1}, resulting in conversions between 4 and 10 %. This level of CO conversion was used to maintain near-differential reactor operation, but still avoiding reduced accuracy of the product analyses caused by too low conversions.

The TCD analyses were taken at 30 to 50 minutes intervals, and one to three FID analyses were taken during each experiment. The experiments lasted for 6 to 24 hours. During the experiments the axial temperature profiles of the catalyst bed were recorded several times to ensure the absence of large temperature gradients.

4 RESULTS AND DISCUSSION

4.1 Characterization of catalysts

4.1.1 Temperature programmed reduction

Hydrogen consumption during the reduction was calculated by using a "calibration factor" found from reduction of Ag_2O, as explained in Chapter 3.2.2. The hydrogen consumption was used to calculate the reduction extent of the metal present: The total hydrogen amount consumed was compared to the amount of hydrogen needed for a complete reduction of the cobalt phases on the calcined catalysts. The total cobalt loading was supposed to exist as Co^{2+} and Co^{3+} ions in the same ratio as in Co_3O_4 when the calculations were done.

In the tables presented in this chapter the hydrogen consumption used to each peak is expressed in terms of [(mol H_2 / mol H_2 needed to a complete reduction of the metal) · 100]. Summation of the hydrogen consumption of the peaks due to cobalt reduction then gives the reduction extent.

When assuming a complete reduction of the different oxidic phases represented by the TPR-peaks, the hydrogen consumption at each peak indicate the amount of the phases present.

4.1.1.1 Influence of calcination temperature

Figure 4-1 shows the TPR spectra of Co/Al_2O_3B (the B denotes the support from Vista) calcined at different temperatures. Figure 4-2 shows the TPR spectra of $CoPt/Al_2O_3B$ calcined at 573 and 648 K, while Figure 4-3 shows the TPR spectrum of Al_2O_3B. Table 4-1 shows the nitrogen content for the same catalysts as in Figure 4-1 and 4-2 calcined at 573 and 648 K. Table 4-2 shows the effect of calcination temperature on degree of reduction for the catalysts, calculated from hydrogen consumption during the TPR runs shown in Figure 4-1. In all the figures the straight line on the X-axis after 1173 K indicates constant temperature.

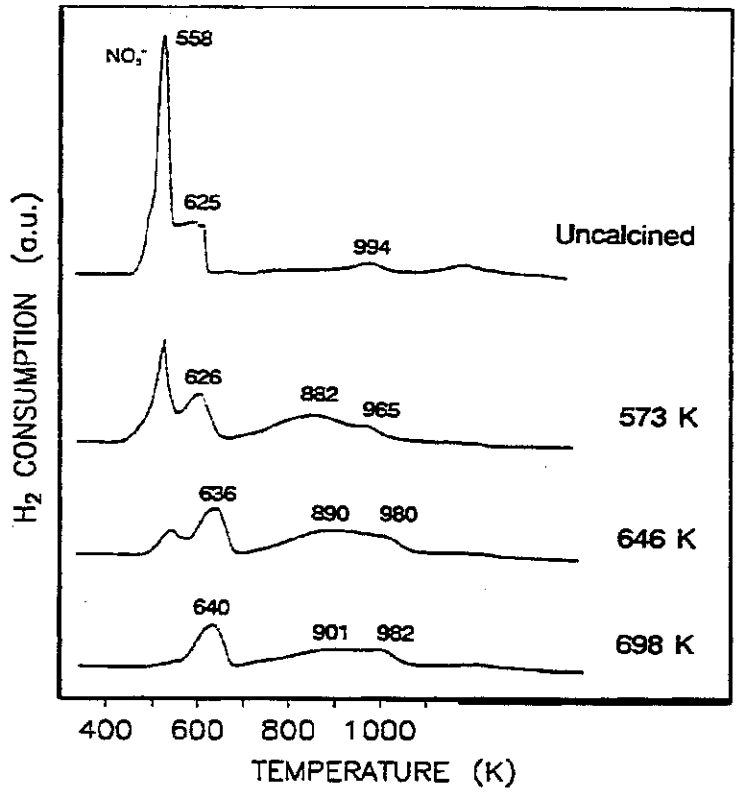

Figure 4-1. TPR spectra of Co/Al_2O_3B calcined two hours at different temperatures. The straight line on the X-axis after 1173 K indicates constant temperature.

Table 4-1. Nitrogen content in catalysts calcined at 573 and 648 K.

Catalyst	Calcination temperature (K)	Nitrogen content (wt %)
Co/Al_2O_3B	573	0.46
Co/Al_2O_3B	648	0.14
$Co1.0Pt/Al_2O_3B$	573	0.50
$Co1.0Pt/Al_2O_3B$	648	0.17

Table 4-2. Effect of calcination temperature on H_2 consumption in reduction of Co/Al_2O_3B (calculated from TPR with 0.2 g of catalyst, 300-1173 K, 10 K/min, 30 ml/min of 7%H_2 in Ar). Calcination time is two hours.

Calcination temperature (K)	H_2 consumption[a]				
	Total (1.+2.+3.)	1st peak (600-650 K)	2nd peak (700-1050 K)	3rd peak (1200 K)	NO_3^- peak[b] (550 K)
Uncalcined	90	38	28	24	85
573	82	24	49	9	25
648	76	23	47	6	10
698	63	21	35	7	2
573 [c]	36	34	2[c]	-	35

[a] Expressed in terms of [(mol H_2 consumed / mol H_2 needed to a complete reduction of the metal)·100].

[b] The stoichiometry for hydrogen consumption in the reductive decomposition of nitrate is not known. This value is for simplicity expressed in terms of % reduction. It can therefore not be used to calculate the degree of decomposition, but only to compare the amount H_2 measured in the peak.

[c] Heating rate 2 K/min, final temperature 623 K, other variables are not changed.

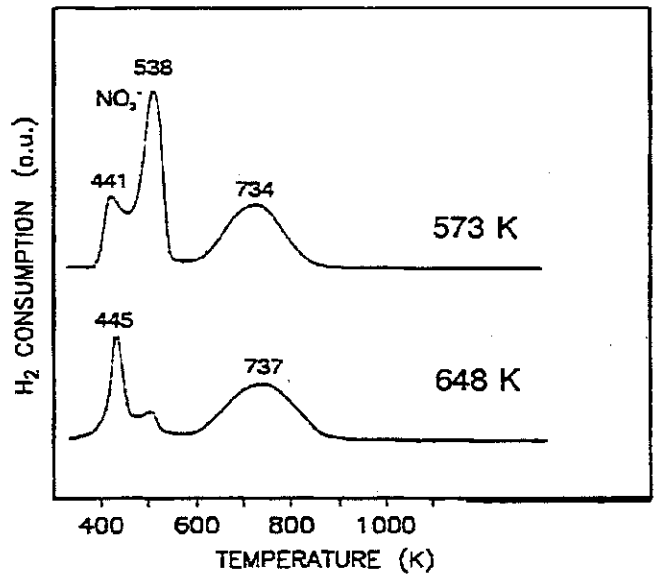

Figure 4-2. TPR spectra of $Co1.0Pt/Al_2O_3B$ calcined two hours at 573 and 648 K.

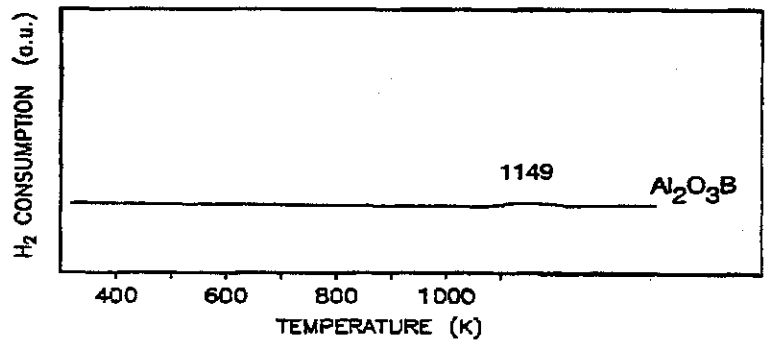

Figure 4-3. TPR spectrum of Al_2O_3B.

The spectra in Figure 4-1 typically consist of three or four peaks: The first appears around 550 K and the second at 600 - 650 K. The third, a broad peak, appears between 700 and 1050 K. This peak has a shoulder and consists most probably of two overlapping peaks. The small fourth peak is seen around 1200 K.

The interpretation of the TPR-spectra shown here is based on the literature discussed in Chapter 2.4.

The large peak around 550 K is for several reasons concluded to be due to a reductive decomposition of cobalt nitrate not complete decomposed during the calcination:

I) The size of the peak decreases with increasing calcination temperature, indicating an increasing degree of decomposition during the calcination. The same nitrate decomposition peak is found for 9%Co/Al_2O_3 by Arnoldy and Moulijn /3/. They could also detect NO and NO_2 from the catalyst sample during TPR experiments with a flame ionization detector (FID). Both their TCD peak (from H_2 consumption) and their FID peak (from NO_x evolution) decreased with increasing calcination temperature, and were not seen for catalysts calcined at temperature above 650 K.

II) Elemental analyses of the catalysts used in this study showed (Table 4-1) decreasing amount of nitrogen with increasing calcination temperature. This confirm that the calcination at low temperatures is incomplete. The nitrogen content of the catalyst calcined

at 573 K is approximately three times the nitrogen content for the catalyst calcined at 648 K. The ratio between the TPR "nitrate" peaks for catalysts calcined at 573 and 648 K (Table 4-2) is in agreement with this result. The values measured for the nitrogen content correspond to approximately 85 % and 95 % decomposition of the initial amount of nitrogen in the cobalt nitrate used for impregnation for Co/Al_2O_3B calcined at 573 and 648 K, respectively.

From the above results and from Figure 4-1 it is obvious that with 2 hours calcination time, a temperature above 648 K is necessary for a complete decomposition of the nitrate on these catalysts.

Guczi et al. /22/ assumed a complete decomposition of cobalt nitrate in oxygen and therefore assigned the two large TPR-peaks (at 520 and 670 K) in the spectrum from $10\%Co/Al_2O_3$ to a two step reduction of Co_3O_4 on surface. Calcination was done for one hour at 573 K. From the discussion above it is likely that the nitrate decomposition was incomplete. Then the first of the two TPR-peaks has to be interpreted as reduction of cobalt nitrate, and not as reduction of Co_3O_4, as suggested by Guczi et al..

In Table 4-1 the same effect of calcination temperature on the nitrate decomposition is seen for a platinum containing cobalt catalyst. The decreasing size of the peak around 510 - 550 K with increasing calcination temperature in Figure 4-2 confirms this result. It is also worth noticing that the addition of platinum does not influence the nitrate decomposition temperature. This could indicate that the decomposition does not require dissociated hydrogen atoms (which is assumed to be the case for cobalt oxide reduction), but instead is a non-catalytical (thermal) process. Further discussion of the effect of platinum addition will be done in Chapter 4.1.1.3.

In accordance with the literature /3,6,9,11,12/, the other low temperature (600 - 650 K) peak in Figure 4-1 is attributed to the reduction of Co_3O_4 particles. A shift to about 15 K higher temperature appears for this peak with increasing calcination temperature from 573 to 698 K. The hydrogen consumption during TPR is shown in Table 4-2. For the peak at 600 - 650 K (reduction of Co_3O_4) it shows a slight decrease with increasing calcination temperature at

constant heating rate. However, this peak overlaps partly with the nitrate decomposition peak. Due to difficulties with separation between the two peaks the decrease could be just an apparent decrease. Then the amount of cobalt as Co_3O_4 particles can be presumed to be constant with increasing calcination temperature at constant heating rate during the reduction.

If the shift in reduction temperature for the Co_3O_4-peak could not be caused by a larger amount of Co_3O_4, a change in the Co_3O_4 particle structure can be suggested to cause the shift. The Co_3O_4 crystallites could have sintered to larger particles during the calcination. If the reduction of "bulky" particles is controlled by H_2 diffusion (assuming the "contracting sphere reduction mechanism" /56/), the reduction rate will depend on the particle size. The TPR peak will accordingly shift to higher temperature with increasing particle size. Okamoto et al. /137/ have shown a distinct increase in the TPR temperature with increasing Co_3O_4 particle size. The increase in TPR temperature was independent of the support (SiO_2, Al_2O_3 or unsupported), which could indicate that the crystalline Co_3O_4 particles on support behave as unsupported bulk Co_3O_4.

To investigate the reduction of the catalysts done before kinetical investigation, some TPR-runs were performed with a heating rate of 2 K/min up to 623 K. The result from this is also shown in Table 4-2. With a slower heating rate the hydrogen consumption increased, indicating more cobalt as Co_3O_4.

A plausible explanation of the increased hydrogen consumption with low heating rate could be: With the low heating rate the cobalt surface Co^{3+} and Co^{2+} ions are allowed to agglomerate and form Co_3O_4 particles. Poels et al. /120/ reported that the dispersion of nickel on Ni/Al_2O_3 catalysts from $Ni(NO_3)_2$, is decreasing with increasing water content in the reduction gas. They suggested that the major mechanism leading to poor metal dispersion is hydrothermal sintering of Ni^{2+} precursors prior to reduction, and that water moisture greatly enhanced the sintering. With 2 K/min instead of 10 K/min a similar process could be assumed to take place to a larger extent on the investigated cobalt catalysts. Water present from the decomposition of cobalt nitrate (and from the first part of the cobalt oxide reduction) will facilitate the process.

The broad peak between 700 and 1050 K is attributed to a surface layer of Co^{2+} and Co^{3+} ions, with reduction of the latter to Co^{2+} responsible for the first part of the peak. This was suggested by Arnoldy and Moulijn /3/ and later confirmed by Tung et al. /11/. It is seen in Table 4-2 that the hydrogen consumption to reduction of this phase decreases simultaneously as the peak in Figure 4-2 shows a tendency to appear at higher temperature. In agreement with Arnoldy and Moulijn /3/ the lower amount of surface Co^{2+} and Co^{3+} can be explained with an increased diffusion of cobalt ions into the alumina lattice. The cobalt ions left on the surface will then have more Al^{3+} neighbors, giving stronger interactions to the support. Then the shift to higher temperature could indirectly also be regarded as caused by the increased diffusion into the alumina lattice.

A weak peak can be recognized around 1170 K and this could be suggested to be due to reduction of a more or less crystalline $CoAl_2O_4$ phase /7,14,Figure 2-4/. But a peak is also observed in this range for pure alumina (Figure 4-3). When heating to temperatures higher than 1170 K γ-Al_2O_3 looses water and becomes δ-Al_2O_3 /65/. The peak at 1170 K in Figure 4-1 can therefore also be the result of an alumina phase transition. On the other hand, for some catalysts the same peak does not appear at all (Figure 4-2), and the 1170 K peak is most probably caused by the reduction of cobalt aluminate. In addition, the size of the peak changes with calcination temperature, and there is a difference between calcined and uncalcined catalysts. This also indicates that the weak peak is due to a cobalt component.

There seems to be a higher degree of formation of the suggested, heavy reducible cobalt $CoAl_2O_4$ phase (3rd peak in Table 4-2) after decomposition of cobalt nitrate in a reducing atmosphere rather than an oxidizing atmosphere. This may be due to the lack of oxidation of the Co^{2+} ions to Co^{3+} ions, and consequently higher degree of Co^{2+} ion diffusion into the octahedral alumina lattice sites. This is confirmed by the lower amount of Co^{2+}/Co^{3+} surface layer for the uncalcined catalyst.

Due to the decrease in the total hydrogen consumption observed in Table 4-2 with increasing calcination temperature, there may be a possibility for some unreduced $CoAl_2O_4$ left in the catalyst after the TPR run. More Al^{3+} ions in the surroundings of the cobalt ions make them considerably less reducible /3/. From this it could be suggested that the observed decrease in

the total hydrogen consumption with increased calcination temperature is due to an increased Co^{2+} diffusion into the alumina lattice, and to a gradually change from an amorphous cobalt-alumina phase to the more crystalline $CoAl_2O_4$. The decrease in reduction extent with increasing calcination temperature is in agreement with the results from XPS investigations reported by Chen and Hercules /7/.

The slight observed decrease in the high temperature reduction peak with an increase in the calcination temperature from 573 to 648 K could be due to the increased decomposition of cobalt nitrate before reduction. This will give relatively lower Co^{2+} concentration and less spinel formation. A minor increase in this reduction peak seen for the highest calcination temperature, can be due to higher Co^{2+} ion diffusion rates at higher temperatures, and thus higher spinel formation. A reservation has to be taken with respect to the small changes discussed for the highest temperature peak: analyses uncertainty could also be a reason to the observed differences between the spectra.

4.1.1.2 Co_3O_4

The effect of the support was investigated by comparing unsupported Co_3O_4 with Co/Al_2O_3B calcined at 648 K. Two different Co_3O_4 materials were used: The first was a commercial Co_3O_4, delivered by Merck and the second was made in the laboratory at NTH by precipitation and calcination as described in Chapter 3.1. The precipitated cobalt salt had a blue-green color before calcination, and this indicates the presence of $CoO*H_2O$ /60/. This compound is easily oxidized to Co_3O_4 /60/ and therefore cobalt was assumed to exist as Co_3O_4 after two hours calcination at 648 or 698 K. A change in color from green to black during calcination supports this assumption.

Figure 4-4 shows the TPR spectra for the three different catalysts. Table 4-3 shows the hydrogen consumption and the peak temperatures during TPR for the two bulk Co_3O_4 materials and their BET surface areas.

In agreement with the literature /3,6,9,79/ the high temperature peak (890 K) observed under reduction of Co/Al_2O_3B (Figure 4-4) is not observed under reduction of unsupported Co_3O_4.

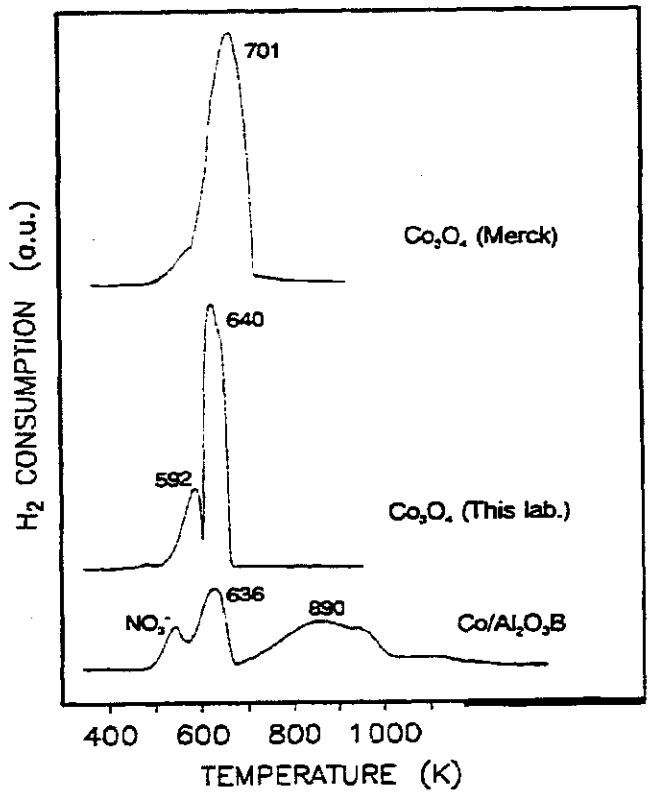

Figure 4-4. TPR spectra of different Co_3O_4 catalysts compared to an alumina supported cobalt catalyst.

Table 4-3. TPR and BET results for Co_3O_4.

Catalyst	Hydrogen consumption[a] (%)		Peak temperature (K)		BET surface (m^2/g)
	1st peak	2nd peak	1st peak	2nd peak	
Co_3O_4(648)[b]	23	77	592	640	-
Co_3O_4(698)[b]	22	78	594	660	22
Co_3O_4(Merck)	6	94	590	701	14

[a] Hydrogen consumption for each peak is expressed in % of the total hydrogen consumption.
[b] The parentheses denotes the calcination temperature.

The peak at 600 - 650 K, earlier interpret to be "bulky" Co_3O_4 is seen on both the supported and the unsupported catalysts. This supports that the low (600 - 650 K) and high (700 - 1050 K) temperature peaks identified in the previous chapter are indeed crystalline Co_3O_4 and well dispersed cobalt interacting with the support surface, respectively.

Investigations done with variation of the amount of cobalt /7,11/ show that cobalt aluminate is the only cobalt phase at 1 wt % cobalt loading. Increasing the cobalt loading gives formation of other phases. After "filling up" the subsurface alumina lattice and then the surface layer with cobalt ions, discrete Co_3O_4 particles are formed from surplus cobalt.

An interesting observation in Figure 4-4 is that the TPR profile is different for the two unsupported Co_3O_4 compounds. In the literature the same difference is found: Both Arnoldy and Moulijn /3/ and Wang and Chen /6/ used commercial Co_3O_4, and their TPR spectra show a single peak. Lapidus et al. /79/ prepared Co_3O_4 by mixing citric acid with a cobalt nitrate solution, followed by calcination at 773 K. The TPR spectrum showed a single peak. Sexton et al. /9/ precipitated cobalt nitrate with an excess of hot potassium carbonate solution, followed by calcination at 623 K. Their TPR spectrum showed two peaks similar to the result in this study. van't Blik and Prins /12/ prepared Co_3O_4 by oxidizing the reduced metal at 1073 K for 72 hours. This resulted in a broad reduction peak with a distinct shoulder on the low temperature side.

An explanation of the two reduction peaks is a two step reduction of Co_3O_4 via CoO to Co metal. This is supported by the ratio between the hydrogen consumption of each step on 23:77, which is close to the theoretical 25:75 (Eq. 20 and 21, Chapter 2.4.1). The broader, single reduction peak for the commercial Co_3O_4 in Figure 4-4 is shifted to higher temperature compared to the two peaks for the NTH made Co_3O_4, and this broad peak must represent both reduction steps, which are overlapping.

Castner et al. /112/ studied the reduction behavior of Co_3O_4 and silica supported cobalt catalysts extensively by a number of methods (XAS, XPS, TEM and TPR). All their results were consistent with the H_2 reduction of Co_3O_4 proceeding to metallic Co via CoO intermediate species.

The reason for the different reduction behavior of the different Co_3O_4 compounds is not known. By comparing the TPR-conditions used in the different investigations /3,6,9,10,12,79/, differences in conditions is unlikely to cause the presence of one or two peaks. But a shift to higher peak temperatures is seen between the catalysts calcined at 648 and 698 K. The shift is accompanied by a slight decrease in the hydrogen consumption ratio between the two peaks. This could indicate that the reduction properties are changing with calcination temperature. The BET surface measurements shown in Table 4-3 indicate larger crystallites for the commercial Co_3O_4 bulk compound compared to the Co_3O_4 made at NTH.

The same overlapping of the two reduction steps as seen on the commercial cobalt oxide is assumed to appear for the reduction of Co_3O_4 on support.

4.1.1.3 Platinum promotion.

Figure 4-5 shows the TPR-spectra from Co/Al_2O_3A, $Co0.1Pt^*/Al_2O_3A$, $Co1.0Pt^*/Al_2O_3A$ and $0.3Pt^*/Al_2O_3A$ (the asterisk denotes chloride-containing platinum-salt and the A denotes support from Akzo). Table 4-4 shows the degree of cobalt reduction of these catalysts.

Figure 4-5 shows that addition of small amounts of platinum to the cobalt catalyst shifts the reduction peaks to lower temperatures. The shift is dependent of the platinum loading: 0.1 wt % platinum addition to Co/Al_2O_3A gives the Co_3O_4-peak a shift of about 140 K from 663 to 526 K, while the second peak is shifted about 100 K from 893 to 788 K. Increased platinum amount to 1 wt% gives the second peak an additional shift of 100 K to 685 K, whereas the first peak remains in almost the same position as with 0.1 wt% platinum.

None of the pronounced peaks in these spectra are due to the reduction of platinum. The atomic ratio between cobalt and platinum on the catalysts is at least 32, and therefore the reduction of platinum is almost undetectable when the apparatus is optimized for the cobalt reduction peaks. In Figure 4-5 a very small reduction peak is observed for $0.3Pt^*/Al_2O_3$ with a peak temperature of 514 K. This reduction temperature is in agreement with other studies /24,61,68,104,105/ of platinum catalysts.

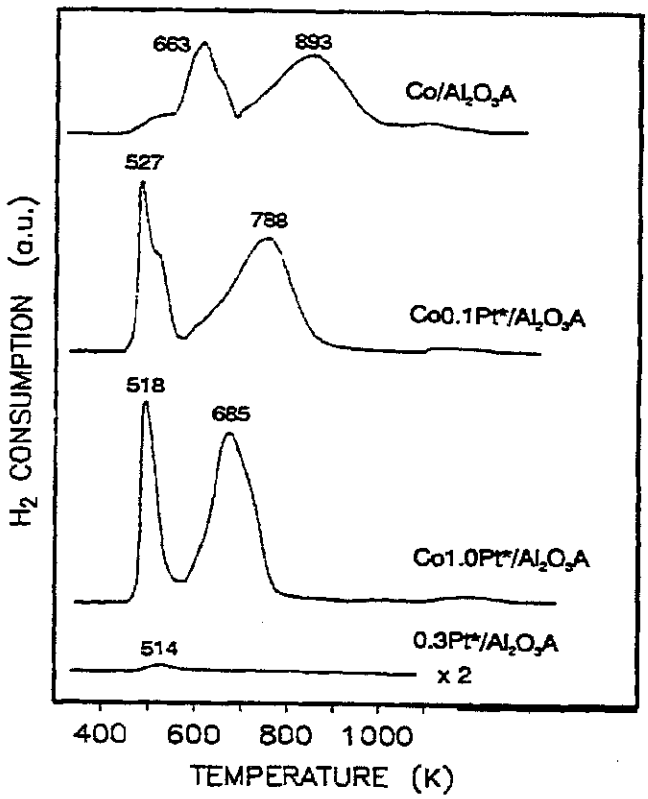

Figure 4-5. TPR-spectra of Co/Al_2O_3A and Co/Al_2O_3A promoted with 0.1 and 1.0 wt % Pt, and $0.3Pt^*/Al_2O_3A$. Calcination temperature 673 K.

Table 4-4. Influence of platinum amount on H_2 consumption in TPR. Calcination temperature 673 K.

Catalyst	H_2 consumption				
	Total (1.+2.+3.)	1st peak	2nd peak	3rd peak	NO_3^{2-} peak
Co/Al_2O_3A	85	27	53	5	4
$Co0.1Pt^*/Al_2O_3A$	95	29	63	3	-
$Co1.0Pt^*/Al_2O_3A$	94	29	62	3	-

From Table 4-4 an apparent increase in the H_2 consumption for both main peaks is seen when platinum is added, but the second peak shows the largest increase. The small third peak shows a slight decrease in H_2 consumption with platinum addition.

The size of the nitrate peak for Co/Al_2O_3A (Table 4-4) corresponds to a hydrogen consumption giving 4 % reduction of the total cobalt amount. The first peak in the spectra from the Co-Pt catalysts (Figure 4-5) overlaps with the nitrate peak. The shoulder observed on the right side of the low temperature peak for $Co0.1Pt^*/Al_2O_3A$ could be due to the nitrate reduction. The minor increase in the H_2 consumption of the first peak of the platinum promoted catalysts in Table 4-4 is therefore most probably due to the overlapping of the Co_3O_4 reduction peak with the nitrate reduction peak, and not a result of a higher amount of Co_3O_4. This is supported by the fact that summation of the H_2 consumption for the separate peaks gives close to 100 % reduction (Table 4-4), assuming the cobalt ions being initially present as in Co_3O_4. This means that a real increase is only seen for the amount of the 2nd peak identified as a cobalt surface phase.

The increase in the amount of surface cobalt could indicate that platinum addition prevent the Co^{2+} diffusion into the alumina lattice. This is supported by the slightly lower H_2 consumption for the 3rd peak around 1200 K, identified as $CoAl_2O_4$, and by the total H_2 consumption corresponding to a reduction close to 100 %.

Guczi et al. /22/ also found platinum promoted shifts in reduction temperature for cobalt catalysts. Matusek et al. /24/ observed the same for platinum promoted ruthenium catalysts. A platinum assisted process is suggested: The minute amount of zerovalent platinum being present at the beginning of the TPR measurements generates hydrogen atoms which facilitate the reduction of cobalt or ruthenium oxide. This seems to be a reasonable explanation of the observed phenomena. The effect is suggested /22/ to be dependent of the size of interface between the two metals. The shift to 518 and 527 K observed for Co_3O_4 reduction in Figure 4-5 is in good agreement with the observed reduction temperature (514 K) for $0.3Pt^*/Al_2O_3$.

Furthermore, Guczi et al. /22/ suggested that a part of the cobalt was not associated with platinum, as indicated by a peak at 670 K for both a pure cobalt catalyst and a platinum-

cobalt catalyst. However, Guczi et al. /22/ did not reduce at temperatures higher than 850 K, and consequently could not observe the reduction peak of the surface phase cobalt for the unpromoted catalyst (the peak at 800 - 1000 K in Figure 4-5). Figure 4-5 shows that the peak just below 700 K for the 1 % Pt promoted and the unpromoted catalyst represent the reduction of two different phases.

4.1.1.4 Promotion with other noble metals

Other (Re, Pd, Ru, Ir) noble metals are also effective in promoting the reduction of cobalt. This is seen from Figure 4-6 and Figure 4-7. The extent of reduction for the catalysts in Figure 4-6 is shown in Table 4-5. The content of second metal in the catalysts in Figure 4-6 is approximately 0.1 wt %, and in the catalysts shown in Figure 4-7 approximately 1 wt%.

The different second metals all give different spectra, but a common feature is the promotion of reduction of the surface phase, represented by the second TPR-peak. At 0.1 wt% loading the ability of the different metals to shift this peak decreases in the order

$$Pt = Ru > Ir > Pd > Re.$$

Table 4-5. H_2 consumption in TPR. Co/Al_2O_3 with 0.1 wt% of different metals. Calcination temperature 673 K.

Catalyst	H_2 consumption				
	Total (1.+2.+3.)	1st peak	2nd peak	3rd peak	NO_3^{2-} peak
Co/Al_2O_3A	85	27	53	5	4
$CoRe/Al_2O_3A$	84	23	60	1	3
$CoPd/Al_2O_3A$	92	32	57	3	-[a]
$CoRu/Al_2O_3A$	88	26	59	3	2
$CoIr/Al_2O_3A$	96	33	60	3	-[a]
$CoPt/Al_2O_3A$	95	29	63	3	-[a]

[a] The peak is overlapping with the 1st cobalt reduction peak, and is impossible to measure.

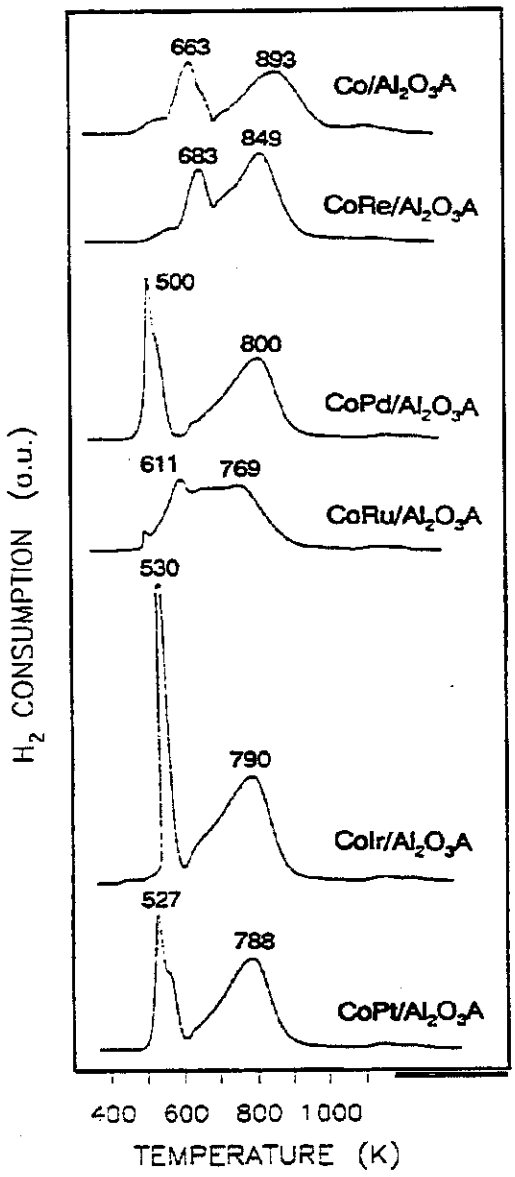

Figure 4-6. **TPR spectra of Co/Al_2O_3A promoted with 0.1 wt% of different metals. Calcination temperature 673 K.**

For the ruthenium promoted catalyst the shape of the peak is markedly different compared to the others: The second peak is much broader, and overlaps with the low temperature peak. In the discussion in Chapter 4.1.1.1 it was suggested that the first part of the 700 - 1050 K peak represented reduction of Co^{3+} to Co^{2+}. The shape of the peak for the ruthenium promoted catalyst could indicate a large content of Co^{3+} surface ions.

The ability of the metals to shift the low temperature peak (Co_3O_4 phase) does not decrease in the same order as for the high temperature peak. In this case the order at 0.1 wt% loading is:

$$Pt = Pd = Ir > Ru >> Re.$$

The results in Figure 4-6 indicate that rhenium does not promote the reduction of this cobalt phase at all, in fact a small increase in the reduction temperature is observed. Similar shifts in the reduction temperatures of the cobalt phases on $10\%Co/Al_2O_3$ are found by Lapidus et al. /118/ when 0.3 wt% of Pd and Ru are added to the catalyst.

Table 4-5 shows that the H_2 consumption is increased for the surface phase (2^{nd} peak) for all the promoted catalysts compared to the unpromoted catalyst. It is also common for the promoted catalysts that the second metal slightly decreases the amount of $CoAl_2O_4$ (3^{rd} peak). As discussed for the platinum promotion, this could indicate that addition of a second metal prevent Co^{2+} diffusion into the alumina lattice. This could be caused by blockade of the alumina by well dispersed noble metal, or by interactions between the cobalt ions and the noble metal.

For some of the catalysts there is an apparent increase in H_2 consumption also for the reduction of the Co_3O_4 phase (1^{st} peak), but this is only observed when this peak overlaps with the nitrate reduction peak. From this the increase in H_2 consumption is suggested to be due to reductive decomposition of nitrate.

In Figure 4-7 the effect of 1 wt% Pt and 1 wt% Re addition to Co/Al_2O_3B is compared. In this figure the TPR-peak due to decomposition of nitrate at 530 - 550 K is pronounced because of the low (573 K) calcination temperature of the catalysts. The high temperature

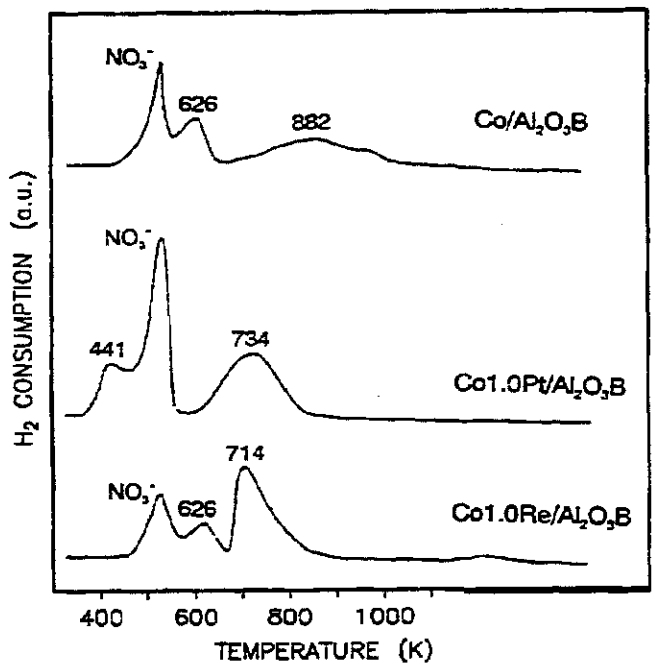

Figure 4-7. TPR-spectra of Co/Al_2O_3B and Co/Al_2O_3B promoted with 1 wt% Pt or 1 wt% Re. Calcination temperature 573 K.

peak has shifted approximately 150 K for both Pt and Re promoted catalysts. But rhenium gives a sharper peak compared to platinum. However, the main difference between the two noble metals is the effect on the reduction of the Co_3O_4 phase (low temperature peak). For the CoPt catalyst a shift of 185 K is observed, while the CoRe catalyst does not differ from the unpromoted Co catalyst in the reduction of the Co_3O_4 phase. It is seen that the peak position remains at 626 K.

In Figure 4-6 the high temperature peak from the 0.1 wt% Re promoted catalyst is shifted approximately 50 K compared to the unpromoted cobalt catalyst. In Figure 4-7 the shift is more than 150 K for the 1 wt% Re promoted catalyst. In Table 4-6 the shift in peak temperatures appearing from different amounts of platinum and rhenium are compared. It is seen that there is an effect of second metal loading for both metals.

Table 4-6. Temperature shift in TPR peaks due to Pt and Re promotion of 10%Co/Al_2O_3.

Second metal loading (wt%)	Shift in 2nd peak (K)		
	Pt	Pt*[a]	Re
0.1	-[b]	105	44
1.0	148	208	168

[a] The asterisk denotes chloride containing platinum precursor.
[b] Not investigated.

van't Blik and Prins /12/ explained a similar promoting effect of rhodium on cobalt reduction by assuming that the initially formed metallic rhodium during the reduction acts as nucleation centers. At these sites hydrogen molecules are dissociated to yield hydrogen atoms which, opposed to hydrogen molecules, are reactive in reduction and consequently reduce the cobalt nitrate (uncalcined catalysts) at lower temperatures. The suggestion of reduction of the promotor as a necessary step before it promotes the cobalt reduction is in agreement with the conclusions of Guczi /22/, and also of Shpiro et al /29/. Literature TPR data /3,12,24,61,62,63,64,147/ showing the reduction temperature of metal oxides and metal nitrates on γ-Al_2O_3 support are given in Table 4-7. Inspection of these data shows that the order of ability to shift the first reduction peak of cobalt catalysts (Figure 4-6) is in close agreement with the order of the reduction temperature for the second metals alone. Some exceptions from this rule can be due to the wide range of catalyst preparation procedures used in the different studies. Small differences in the amount of the second metal in this study could also disturb the correlation. Unfortunately, exact analyses of the content of the second metal are not available for the catalysts shown in Figure 4-6. None of these catalysts contain more than 0.1 wt% of the second metal, but e.g. moisture in the metal precursors could have caused lower 2nd metal loading than assumed during preparation of the catalysts.

Platinum, palladium, iridium and ruthenium oxide /24,61,63,64,147/ are all reduced at lower temperature compared to cobalt and rhenium oxides on γ-Al_2O_3. Rhenium oxide /61,62/ seems to be reduced at temperatures between the reduction temperature for the "easy" and the "heavy" reducible cobalt phases /3,12/. This explains why rhenium promotion gives a shift

Table 4-7. Literature TPR data showing reduction temperatures (reduction peak maxima) of supported metal oxides.

Catalyst[a]	Calcination temperature (K)	Reduction temperature(s) (K)		Ref.
0.5%Pt/Al_2O_3	523	381	657	Faro et al. /63/
3%Pt/Al_2O_3	673	400		Subramanian and Schwarz /64/
0.6%Pt/Al_2O_3	833	537		Barbier et al. /68/
0.3%Pt/Al_2O_3	Unknown	573		Isaacs & Petersen /61/
10%Pt/Al_2O_3	Uncalcined	550		Matusek et al. /24/
10%PtRu/Al_2O_3	Uncalcined	490	550	/24/
10%Ru/Al_2O_3	Uncalcined	490	605	/24/
1%Pd/Al_2O_3	673	340		Chang et al. /147/
0.5%Ir/Al_2O_3	523	433	697	/63/
3%Ir/Al_2O_3	673	460		/64/
2.3%Rh/Al_2O_3	Uncalcined	363		van't Blik & Prins /12/
CoRh/Al_2O_3	Uncalcined	413		/12/
4.4%Co/Al_2O_3	Uncalcined	543		/12/
9%Co/Al_2O_3	625	575	875	Arnoldy & Moulijn /3/
0.3%Re/Al_2O_3	575	710		Arnoldy et al. /62/
0.3%Re/Al_2O_3	Unknown	876		/61/
1.3%Re/Al_2O_3	773	710		Vuurman et al. /117/

[a] Metal loading is given in wt%.

to the last cobalt reduction peak, but not to the first.

Other properties of the second metals than the reducibility can also lead to the observed differences in the shifts of the TPR peaks by the different noble metals. The electronic and physical properties of the metals, and their interaction with cobalt must be studied in more details before conclusions about this can be drawn.

A promotional effect of the second metals on the reduction of the Co^{2+}/Co^{3+} surface layer,

and a clear increase in the effect with higher loading of Pt and Re is observed. From this it could be suggested that the oxidic cobalt layer on the support surface is "diluted" by the second metal, or that the second metal is well spread over the oxidic cobalt layer. With increasing loading or increasing dispersion of the second metal the promotional effect on the cobalt reduction will increase. The differences in temperature shifts on reduction of the oxidic cobalt layer at constant second metal loading, could indicate differences in the dispersion of the second metals.

Not only the shift, but also the shape of the second reduction peak is changing as the second metal loading increases. This is seen for platinum promotion in Figure 4-5 and for rhenium promotion by comparing the TPR spectra from rhenium promoted catalysts in Figure 4-6 (0.1 wt%) and in Figure 4-7 (1 wt%). The second cobalt reduction peak becomes sharper and more symmetric and the shoulders disappear with increasing amount of Pt or Re. An additional effect of the noble metal can be oxidation of Co^{2+} ions to Co^{3+} ions during calcination as suggested by Sass et al. /19/ after investigation of palladium promoted, reduced and reoxidized cobalt catalysts by ESR and optical spectroscopy. This will be in agreement with the observed, lower extent of Co^{2+} diffusion into the alumina lattice for promoted catalysts. As discussed earlier a tendency for higher Co^{3+} content is seen for ruthenium even at small loadings (Figure 4-6).

4.1.1.5 Reduction at standard conditions

The promotional effect of platinum and rhenium during the reduction at standard conditions used in activity and chemisorption tests is shown in Figure 4-8. In this case the catalysts were reduced like they were before the activity and chemisorption tests (2 K/min, 623 K for 16 hours in pure hydrogen). They were then flushed in argon and cooled down to ambient temperatures, before an ordinary TPR run was performed.

TPR of the pre-reduced Co/Al_2O_3B does not give any low temperature peaks, but a broad high temperature (800 - 1000 K) peak due to reduction of the oxidic surface layer appears. It is clear that mainly the Co_3O_4 phase is reduced in the cobalt catalyst during the pre-

reduction at 623 K. TPR of the pre-reduced Pt and Re promoted catalysts do not show any pronounced peaks at all. but a small hydrogen consumption is detected in the high temperature area (800 - 1200 K). This result indicates that both the Co_3O_4 phase and most of the oxidic surface layer are reduced in the cobalt-platinum and the cobalt-rhenium catalysts during the pre-reduction.

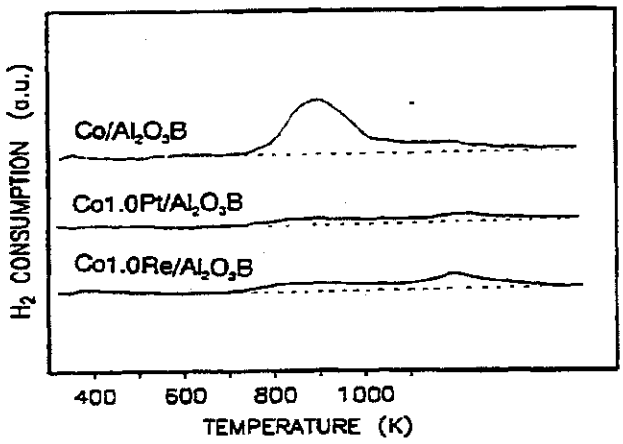

Figure 4-8. TPR of Co/Al_2O_3B and Co/Al_2O_3B promoted with 1 wt% Pt or 1 wt% Re after standard reduction at 623 K for 16 h and cooling to ambient temperature.

4.1.1.6 Effect of chloride containing platinum precursors

The first cobalt reduction peak in the spectrum from $Co1.0Pt/Al_2O_3B$ (chloride free Pt precursor, support from Vista) in Figure 4-7 is observed at 441 K. This is about 80 K lower compared to the $Co1.0Pt^*/Al_2O_3A$ (chloride containing Pt precursor, support from Akzo) shown in Figure 4-5. Two platinum promoted catalysts prepared from two different platinum precursor, $H_2PtCl_6{*}6H_2O$ and $Pt(NH_3)_4(NO_3)_2$, on the same support were therefore compared to investigate if the difference in reduction temperature is due to the platinum precursors. The catalysts were calcined at 673 K. Figure 4-9 shows the TPR-spectra of a platinum promoted catalyst with chloride (Pt*) and a chloride free platinum promoted catalyst (Pt), compared

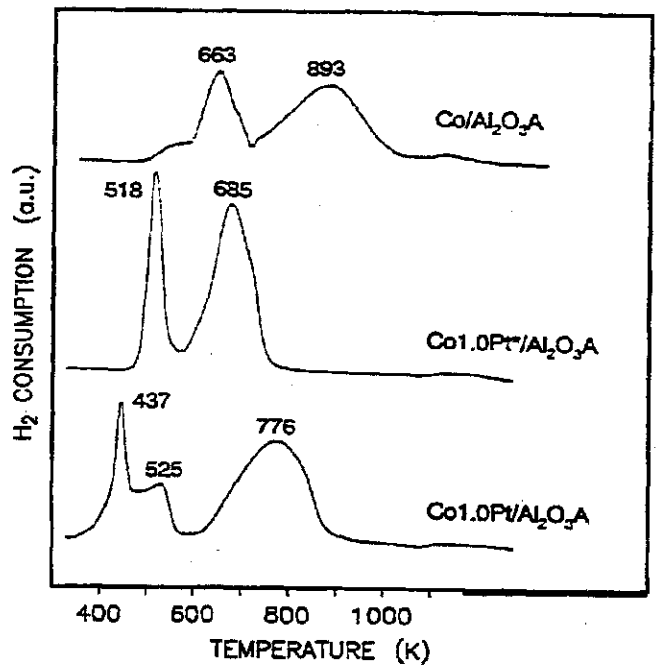

Figure 4-9. TPR-spectra of Co/Al_2O_3A and $Co1.0Pt/Al_2O_3A$ catalysts with chloride (Pt*) and without chloride (Pt). Calcination temperature 673 K.

with an unpromoted cobalt catalyst.

The small peak seen at about 525 K for the chloride free CoPt catalyst is assumed to be due to reductive decomposition of nitrate residuals. The same peak is also seen for Co/Al_2O_3A, but for the chloride containing CoPt catalyst this peak is overlapping with the first large peak at 518 K.

A 80 K shift between the low temperature peaks (Co_3O_4 reduction) for the platinum promoted catalysts is also observed in Figure 4-9. Another difference observed between the two Pt-promoted catalysts is that the high temperature peak (oxidic cobalt layer) is broader for the chloride free catalyst compared to the chloride containing platinum catalyst. In contrast to the low temperature peak, the chloride containing platinum catalyst shows a larger downward

shift of the high temperature peak compared to the Co/Al_2O_3A catalyst.

Chloride ions can /65/ exchange with hydroxyl groups on the support. Lieske et al. /67/ have shown the existence of chloride complexes, $[Pt^{IV}O_xCl_y]_s$, in Pt/Al_2O_3 catalysts. These complexes are reported to be present after several reductions and reoxidations /67/. Elemental analysis of chloride on calcined $Co1.0Pt^*/Al_2O_3A$ shows that they do not loss chloride during calcination (Appendix 1). Figure 4-10 shows exchange reactions that may occur during the platinum impregnation, leading to the formation of oxychloride of platinum and chloride/ hydroxyl ion exchange /72/.

Pt/Al_2O_3 catalysts made from chloride free precursors were found to be reduced at lower temperatures than catalysts made from chloride containing precursors /67/. The reduction temperature of platinum on alumina support is also dependent of the chloride content of the catalyst /66/. This was explained by formation of oxychloride of platinum. Such species are thermally stable and can only be reduced at high temperatures /67.68/.

Different platinum reduction temperature for the different platinum promoted catalyst due to formation of oxichlorides of platinum could explain the differences in the shifts for the first

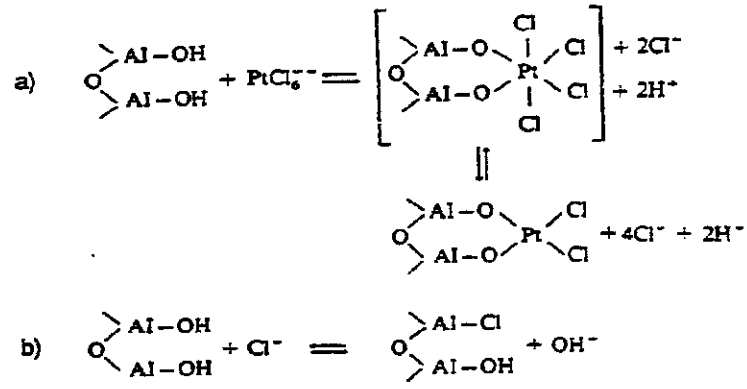

Figure 4-10. Exchange reactions that occur during the impregnation of platinum on alumina. a) Formation of oxychloride of platinum. b) Chloride/hydroxyl ion exchange. From Franck /72/.

cobalt reduction peak (Co_3O_4). This idea is in agreement with the theories suggested in Chapter 4.1.1.3 about the different promoting effect of different second metals: The promoting effect is only observed in the presence of a reduced promoting metal.

Another explanation of the differences in the first peak shift, could be connected to hydrogen transport on support surface: If platinum clusters are separated from the Co_3O_4 particles on the support, the hydrogen molecules dissociated on the reduced platinum will have to move over the support before they are able to reduce the cobalt oxide particles. It is known that hydrogen transport on the support is dependent on the density of hydroxyl groups /65/. A decrease in number of hydroxyl groups on support, caused by chloride ion exchange, will lead to decreased hydrogen transport and could therefore explain why chloride containing cobalt/platinum catalysts give a smaller shift in cobalt reduction temperature compared to the cobalt/platinum catalysts without chloride.

The two different explanations for the observed differences in the first peak shift are not in disagreement with each other, but the last theory requires complete separation between the Co_3O_4 particles and the platinum phases on the support. As referred to in Chapter 2.4.5 SIMS and EXAFS investigations of bimetallic catalyst systems /22,26,29/ give evidence for the existence of bimetallic particles or clusters. If bimetallic particles are formed in the catalysts used in this study, the promoting effect will be independent of hydrogen transport over the support surface. The present investigation does not provide independent evidence for, or against, the existence of bimetallic particles.

However, the different platinum reduction temperatures or retarded hydrogen transport due to chloride ion exchange do not explain why the chloride containing catalyst gives a larger shift to the high temperature cobalt reduction peak compared to the chloride free catalyst. In this case one possible explanation could be that the reduced oxichlorides of platinum are better dispersed /68/ compared to the reduced platinum oxides formed after calcination/ reduction of $Pt(NH_3)_4(NO_3)_2$ /68,106/. The effect of this will be similar to the effect of increased platinum amount seen in Figure 4-5.

4.1.1.7 Summary of the TPR results

- TPR spectra of 9wt%Co/Al_2O_3 catalysts show that the catalysts contain two main cobalt phases. A low temperature (600-650 K) reduction peak is attributed to the reduction of crystalline Co_3O_4 particles. A high temperature (800-1000 K) reduction peak is concluded to represent the reduction of a well dispersed cobalt oxide layer in close contact with the support surface. A small third peak is assumed to represent the reduction of $CoAl_2O_4$.

- The decomposition of cobalt nitrate is incomplete after a two hour calcination at calcination temperatures below 698 K. The reduction of nitrate is represented by a TPR-peak at 510 - 560 K.

- 20 - 35 % of the cobalt in the catalysts calcined between 573 and 698 K are present as Co_3O_4, and about 40 - 50 % is present as an oxidic layer on the support surface.

- The amount of the oxidic cobalt layer is decreasing with increasing calcination temperature, most probably due to Co^{2+} diffusion into the alumina lattice. The total hydrogen content is decreasing with increasing calcination temperature, indicating increasing amounts of $CoAl_2O_4$ left unreduced after the TPR.

- Addition of small amounts of platinum results in lower reduction temperature for both main cobalt phases. The temperature shift is dependent of the platinum loading. Platinum addition does also cause increased amounts of cobalt oxide on the support surface.

- Addition of Ir, Re, Rn and Pd also gives lower cobalt reduction temperatures, but the temperature shifts are not the same for the different metals. It is suggested that the second metal has to be reduced before it promote the reduction of cobalt. Dissociation of hydrogen molecules at the reduced second metal surface probably facilitates the cobalt reduction.

- Catalysts prepared from chloride containing platinum precursors show a different promoting effect compared to catalysts prepared from chloride free platinum precursors.

This is explained with the formation of heavily reducible oxychloride of platinum. The higher reduction temperature of these species results in higher reduction temperature for Co_3O_4 particles. But the oxychloride gives well dispersed platinum, and thus the reduction temperature of the cobalt surface phase becomes lower than was the case for chloride free cobalt platinum catalysts.

In Figure 4-11 a possible picture of the catalyst surface is shown for calcined and reduced cobalt catalysts, with and without a platinum promoter. This is a simplified model, showing the metal and the metal oxide phases which are most probable in view of the results presented and discussed above.

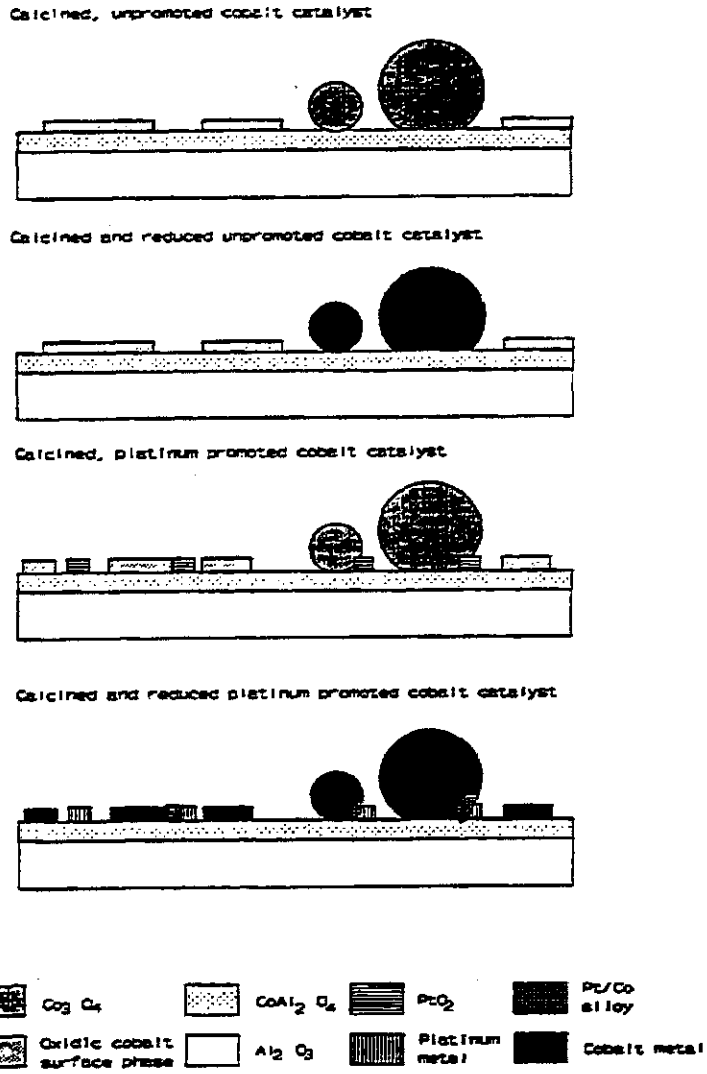

Figure 4-11. A simplified model showing the possible metal/metal oxide phases on calcined and reduced Al_2O_3 supported cobalt catalysts, with and without a platinum promoter.